Synchronizability of two neurons with switching in the coupling

Fatemeh Parastesh [a], Hamed Azarnoush [a], Sajad Jafari [a], Boshra Hatef [b], Matjaž Perc [c,d,*], Robert Repnik [c]

[a] *Department of Biomedical Engineering, Amirkabir University of Technology, 424 Hafez Ave., Tehran, Iran*
[b] *Neuroscience Research Center, Baqiyatallah University of Medical Sciences, Tehran, Iran*
[c] *Faculty of Natural Sciences and Mathematics, University of Maribor, Koroška cesta 160, SI-2000, Maribor, Slovenia*
[d] *Complexity Science Hub Vienna, Josefstädterstraße 39, A-1080, Vienna, Austria*

ARTICLE INFO

ABSTRACT

Time-varying networks are prominently present in the nervous system, where the connections between neurons vary according to the activity of pre and post synapses. Using this as motivation, we here consider a system of two ephaptically coupled neurons with a periodically time-varying link between the two membrane potentials. We derive the master stability function in dependence on the membrane potential coupling strength and in dependence on the ephaptic coupling strength. We first determine coupling ranges at which the two neurons are synchronizable if the link between them is static. In doing so, we find that the ephaptic coupling has a negligible impact on synchronization, while the coupling through the membrane potential has a strong effect. We then consider switching in the coupling, determining the average synchronization error for a fixed ephaptic coupling strength and different membrane potential coupling strengths, and for various switching frequencies. We find the values of the switching coefficient that can synchronize the two neurons for each of the considered switching frequencies, and finally, we also use the basin stability method to determine the global stability of synchronization.

© 2019 Elsevier Inc. All rights reserved.

1. Introduction

Complex networks are helpful tools for clarifying different characteristics of the complex systems [1–4]. Synchronization is a universal phenomenon in complex networks which has been investigated in different physical, chemical and biological networks [5–9]. In the past years, synchronous activity has been discussed extensively in neuronal networks [10–13]. It has been revealed that synchronization of bursting neurons is associated with various cognitive functions and pathological brain states. As examples we can mention Parkinson's disease, essential tremor and epilepsies. Also synchronization of bursting neurons has an important role in processing information of healthy neural tissues [14,15].

The connections between network components are of great significance [16]. Majority of the previous research has studied the synchronization phenomenon in the networks with static coupling [17–19]. But in reality the networks, e.g., biological, epidemiological and social networks, have time varying coupling schemes [20]. In recent years, a few studies have considered the network topologies which vary by time [20–24]. In 2004, Belykh et al. [25] proposed blinking network that

the couplings are independently switched with a predefined probability at specific time duration. Zhou et al. [26] considered a time varying network with slow-switching structure and studied the necessary conditions for synchronization. Stilwell et al. [27] showed that a network with time-varying topology is synchronizable if the network synchronizes for the static time-average of the topology if the time-average can be achieved fast. Buscarino et al. [28] considered a system of two Rössler oscillators with a switching coupling and studied its dynamics with respect to the switching frequency. Rakshit et al. [29] considered a two-layer neuronal network where the intralayer connections switched randomly by time with a specific rewiring frequency. They studied the network synchronization and derived the master stability function.

In the brain, the connections between the neurons depend on the usage of the dendrites and flow of neurotransmitter and therefore is time dependent [30]. Alterations in synaptic strength or connectivity and changes in the excitability of neurons, determine plasticity in neurons [31]. Plasticity exists in spinal dorsal horn neurons, peripheral nociceptors and the brain. It occurs at different levels [32]. At low levels, plasticity occurs in the behavior of single ion channels and at high levels, it can be found in morphology of neurons and large networks [31]. Changes in synaptic strength and synapse number is the most prominent among all the forms of brain plasticity [33]. Timing of activation of presynaptic and post-synaptic activity determines the induction of plasticity [31]. The synaptic plasticity time scales have a wide range of milliseconds to days [26]. Synaptic plasticity has crucial roles in many brain functions, including learning, memory, altering excitability in the brain, regulating behavioral states such as the transitions between sleep and wakeful activity. It is also observed in pathological pain, consisting the inflammation induced by tissue injury and neuropathic pain induced by nerve injury [31,32,34].

One of the other factors that can induce synaptic plasticity is the electric field interactions known as ephaptic coupling. The electrodiffusion within the synaptic cleft induces local electric fields which can change the membrane potential of the presynaptic terminal and therefore the ionic flux. Then the neurotransmitter release is increased. The neurotransmitter release changes the spiking of neurons and influences synaptic strength of two synaptically connected neurons by inducing plasticity [35]. It has been proven that ephaptic interaction affects propagation velocity with reverse relation to gap junctional conductivity [36]. Ephaptic coupling can also lead the independently stimulated axons to become synchronous [37].

In order to better understand the effects of time-varying coupling strength on synchronization, in this paper we consider two coupled neurons in which the coupling strength switches between two different values at a specified frequency. For each neuron we use modified Hindmarsh–Rose model with electromagnetic induction and the two neurons are also coupled ephaptically.

The structure of the paper is as follows: The following section investigates the dynamical model of the system and the coupled network. Section 3 describes the methods and our main numerical results. Finally, the conclusions are presented in Section 4.

2. Model

In 2016, Lv et al. [38] proposed a modified Hindmarsh–Rose model to describe the effect of electromagnetic induction on neuronal activities. The equations of this model are given by:

$$\dot{x} = y + b\,x^2 - a\,x^3 - z + I_{ext} - k_1\rho(\emptyset)x$$
$$\dot{y} = c - d\,x^2 - y$$
$$\dot{z} = r\,[s\,(x + 1.6) - z]$$
$$\dot{\emptyset} = x - k_2\,\emptyset \tag{1}$$

where the variables x, y, z, $\emptyset$ and I_{ext} represent the membrane potential, current for recovery variable, slow adaption current, magnetic flux across membrane and the external forcing current, respectively. The term $\rho(\emptyset) = \alpha + 3\beta\phi^2$ describes the memory conductance of a magnetic flux associated with memory. The parameters are selected as $a = 1$, $b = 3$, $c = 1$, $d = 5$, $r = 0.006$, $s = 4$, $k_1 = 1$, $k_2 = 0.5$, $\alpha = 0.1$ and $\beta = 0.02$. I_{ext} is fixed at 3.4, in which the neuron exhibits chaotic behavior. Fig. 1 shows time series of membrane potential and the attractor of this model at the mentioned parameters.

Firstly, we construct a system consisting of two statically coupled neurons with both membrane potential and ephaptic couplings:

$$\dot{x}_1 = y_1 + b\,x_1^2 - a\,x_1^3 - z_1 + I_{ext} - k_1\rho(\emptyset_1)x_1 + d_x(x_2 - x_1)$$
$$\dot{y}_1 = c - d\,x_1^2 - y_1$$
$$\dot{z}_1 = r\,[s\,(x_1 + 1.6) - z_1]$$
$$\dot{\emptyset}_1 = x_1 - k_2\,\emptyset_1 + d_\emptyset(\emptyset_2 - \emptyset_1)$$
$$\dot{x}_2 = y_2 + b\,x_2^2 - a\,x_2^3 - z_2 + I_{ext} - k_1\rho(\emptyset_2)x_2 + d_x(x_1 - x_2)$$
$$\dot{y}_2 = c - d\,x_2^2 - y_2$$
$$\dot{z}_2 = r\,[s\,(x_2 + 1.6) - z_2]$$
$$\dot{\emptyset}_2 = x_2 - k_2\,\emptyset_2 + d_\emptyset(\emptyset_1 - \emptyset_2) \tag{2}$$

where the subscripts indicate the two respective neurons, d_x is the x variable coupling strength and $d_\emptyset$ is the ephaptic coupling strength. Then we change the x variable coupling to a time-varying link given by $d_x(t) = d_1 + \frac{d_2 - d_1}{2}(sgn\,(\cos(\omega t) + 1)$,
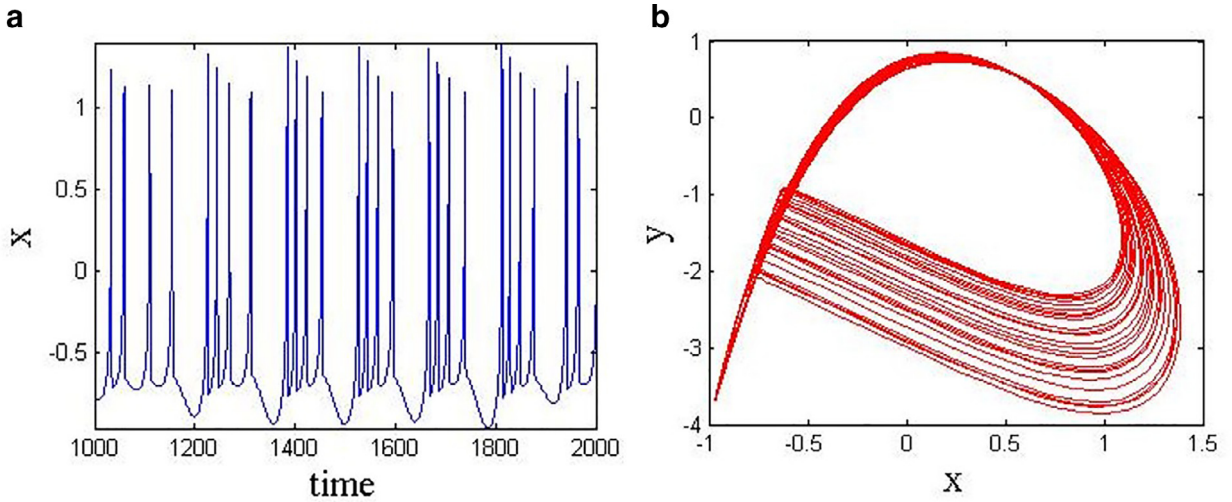
a

b

Fig. 1. (a) The time series of membrane potential of neuron described in Eq. (1) and (b) its attractor in $x-y$ plane for the defined parameters. It can be observed that a single uncoupled neuron exhibit FHC bursting behavior at the defined parameters.

where $sgn(x) = 1$ for $x > 0$ and $sgn(x) = -1$ otherwise. Thus the effective coupling switches between two constant values of d_1 and d_2 at frequency ω.

3. Methods and results

Master stability function (MSF) is a method for finding the conditions that guarantee synchronization of a network of identical nonlinear oscillators [39]. Here at first we apply MSF to the static coupled network to find the coupling strengths ranges where two neurons are synchronizable. To compute MSF, suppose that X_i is the m-dimensional vector of dynamical variables of ith node, $\dot{X_i}= F(X_i)$ is the uncoupled dynamics of the system, and H is the function of each node's variables used in the coupling. Then the dynamics of each node can be described as $\dot{X_i} = F(X_i) + \sigma \sum_j G_{ij} H(X_j)$ where σ is the coupling strength and G relates to the connectivity type. Now the corresponding generic variational equation is defined by $\dot{\xi_k}= [DF+ \sigma \gamma_k DH]\xi_k$ where γ_k is an eigenvalue of G, $k = 0, 1, \ldots, N$. For $k = 0$, the variational equation is along the synchronization manifold and the other ks are related to the transverse eigenmodes of such manifold. Thus, the stability of the synchronous evolution can be obtained by the computation of the maximum Lyapunov exponent of generic variational equation as a function of σ, which is defined as MSF [40].

Hence for the system of Eq. (2), we have:

$$DF = \begin{bmatrix} 2bx - 3ax^2 - k_1\rho(\emptyset) & 1 & -1 & -6k_1\beta\emptyset x \\ -2dx & -1 & 0 & 0 \\ rs & 0 & -r & 0 \\ 1 & 0 & 0 & -k_2 \end{bmatrix}$$

$$H = \begin{bmatrix} 1 & 0 & 0 & 0 \\ 0 & 0 & 0 & 0 \\ 0 & 0 & 0 & 0 \\ 0 & 0 & 0 & 1 \end{bmatrix}, G = \begin{bmatrix} -1 & 1 \\ 1 & -1 \end{bmatrix} \rightarrow \gamma_0 = 0, \gamma_1 = -2 \tag{3}$$

So the variational equation is described as:

$$\dot{\xi_1} = (2bx - 3ax^2 - k_1\rho(\emptyset) - 2\sigma_1)\,\xi_1 + \xi_2 - \xi_3 - (6k_1\beta\emptyset x)\xi_4$$
$$\dot{\xi_2} = -2dx\,\xi_1 - \xi_2$$
$$\dot{\xi_3} = rs\,\xi_1 - r\xi_3$$
$$\dot{\xi_4} = \xi_1 - (k_2 + 2\sigma_2)\xi_4 \tag{4}$$

The maximum Lyapunov exponent of Eq. (4) is computed for different coupling strengths. Fig. 2(a) shows the MSF with respect to d_x and $d_\emptyset$. The black curve in the figure separates the positive and negative values. As can be seen, ephaptic coupling has a much smaller effect on synchronization in comparison with d_x. For each value of $d_\emptyset$, there is a threshold for d_x. If d_x gets higher than that threshold, the system will be synchronous. Changing the value of $d_\emptyset$ from 0 to 2, increases this threshold a bit. Fig. 2(b) shows the MSF for $d_\emptyset = 0.5$. When $d_x < 0.515$, MSF becomes positive and therefore the system is not synchronizable. When $d_x > 0.515$, MSF becomes negative and synchronization occurs.
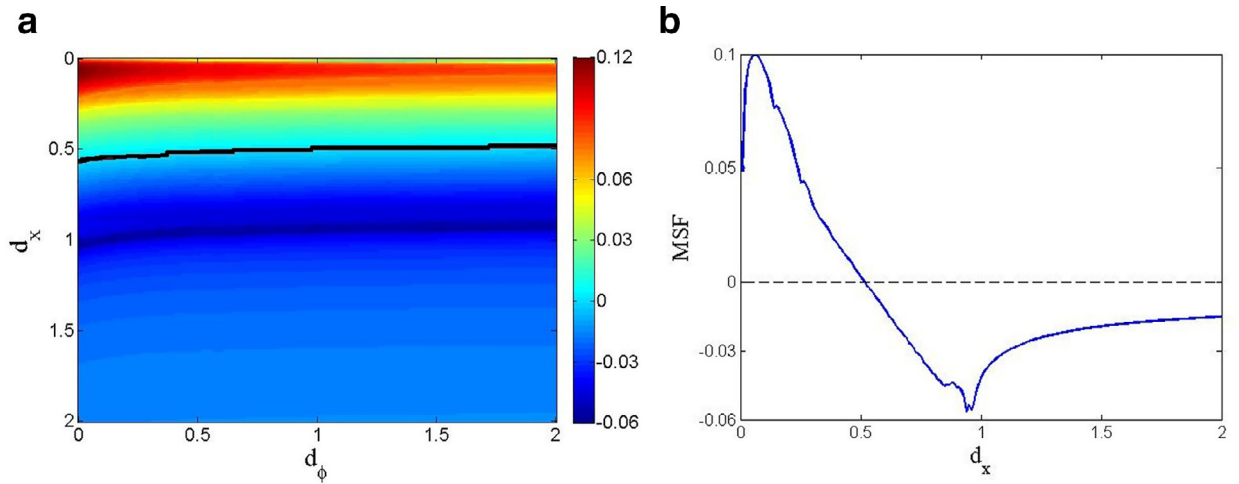
a

b

Fig. 2. (a) 2-D master Stability Function of the system with static coupling with respect to d_x and $d_\emptyset$. It shows the effects of varying the coupling strengths on synchronization. The black line separates the positive and negative MSF values which relate to asynchronizable and synchronizable areas, respectively. (b) 1-D master stability function of the system for $d_\emptyset = 0.5$ with respect to d_x. It shows that the system is synchronizable for $d_x > 0.512$.
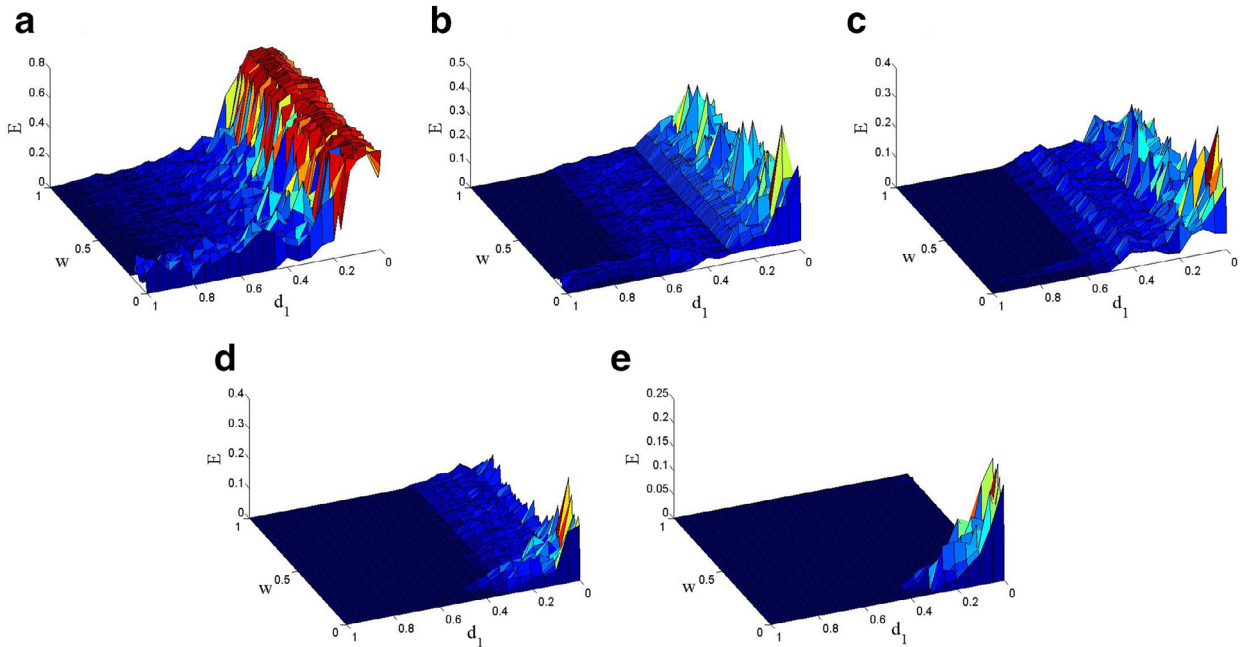
a

b

c

d

e

Fig. 3. Average synchronization error $E(\omega)$ with respect to d_1 and ω, for (a) $d_2 = 0.05$, (b) $d_2 = 0.3$, (c) $d_2 = 0.4$, (d) $d_2 = 0.65$ and (e) $d_2 = 1$. It can be observed that by increasing d_2 value, $E(\omega)$ drops near zero for lower d_1 and ω values, following that the system becomes synchronizable in more extensive region of d_1 and ω.

Now d_x is exchanged with switching coupling and synchronizability is investigated by varying the values of d_1, d_2 and ω. In order to quantify the error of two trajectories with M samples, the average synchronization error $E(\omega)$, is calculated as [28]:

$$E(\omega) = \sum_{h=1}^{M} \frac{\sqrt{(x_1(h) - x_2(h))^2 + (y_1(h) - y_2(h))^2 + (z_1(h) - z_2(h))^2 + (\emptyset_1(h) - \emptyset_2(h))^2}}{\sqrt{x_1(h)^2 + y_1(h)^2 + z_1(h)^2 + \emptyset_1(h)^2 + x_2(h)^2 + y_2(h)^2 + z_2(h)^2 + \emptyset_2(h)^2}} \tag{5}$$

The average synchronization error is computed and normalized in different cases, so that $E \to 0$ corresponds to the synchronous state. Fig. 3 shows the synchronization error ($E(\omega)$) for different d_2 values with respect to d_1 and ω. In Fig. 3(a) d_2 is fixed at 0.05. When the value of d_1 is small, the system is asynchronous for all values of switching frequencies. When d_1 is increased, higher values of ω can synchronize the system. The same average error with wider synchronization region is seen until $d_2 = 0.3$. For $d_2 = 0.3$, when $d_1 < 0.6$, the system is not synchronous for any values of ω and when $d_1 > 0.6$, the
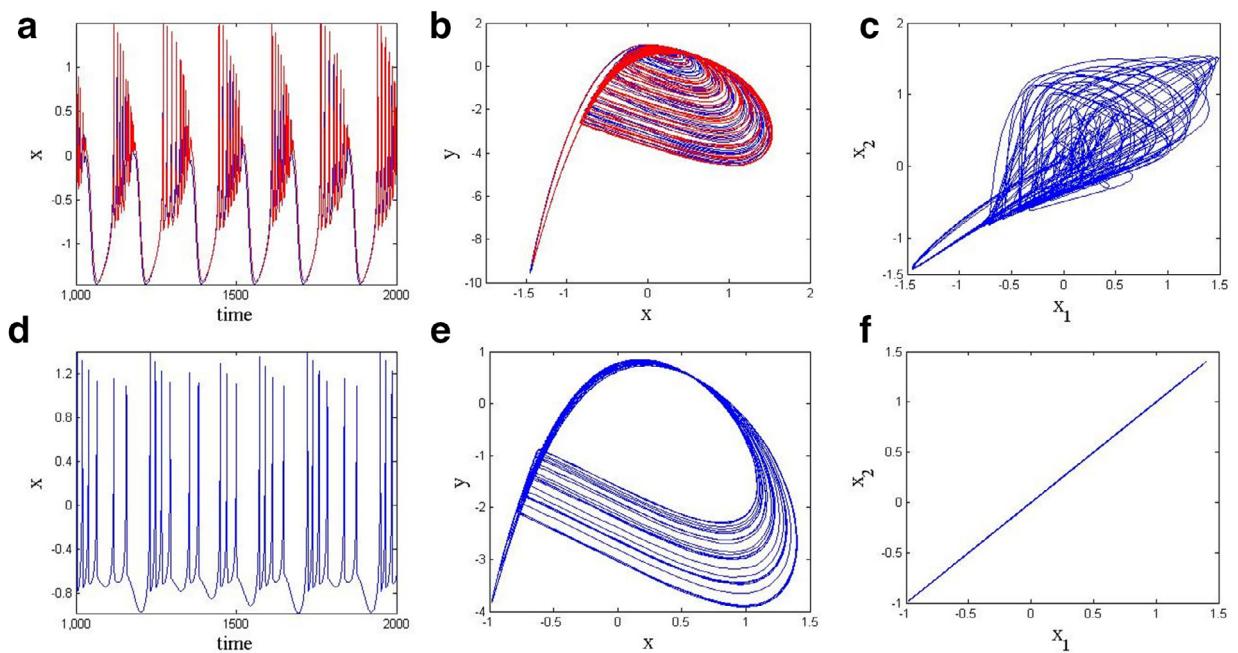
Fig. 4. The first row shows asynchronous state, in this case the neurons show FH bursting behavior: (a) The time series of membrane potential of first and second neurons (colored in blue and red, respectively), (b) the projections of attractors in the $x - y$ plane and (c) projection of attractor in the $x_1 - x_2$ plane. The second row shows synchronous state, in this case the neurons show FHC bursting behavior: (d) The time series of membrane potential of first and second neurons (colored in blue and red, respectively), (e) the projections of attractors in the $x - y$ plane and (f) projection of attractor in the $x_1 - x_2$ plane. (For interpretation of the references to color in this figure legend, the reader is referred to the web version of this article.)

system is synchronous for most of ω values, but there is a peak in $E(\omega)$ around $\omega = 0.1$, as can be seen in Fig. 3(b). When d_2 reaches 0.4 (Fig. 3(c)), the system becomes synchronous for $d_1 > 0.5$ and all ω values. Further increase of d_2, reduces the value of d_1 above which the system is synchronous. But still there are some errors for small d_1 and ω around 0.1, as can be seen for $d_2 = 0.65$ in Fig. 3(d). Raising d_2 to higher values causes the system be asynchronous just for small d_1 and ω around 0.1 as can be seen for $d_2 = 1$ in Fig. 3(e).

Considering time series of the system in different coupling parameters shows that varying the coupling strengths or frequency do not change the behavior of the neurons from chaotic bursting to periodic, although there is a difference between synchronous and asynchronous states. Fig. 4 depicts time series and attractors of two neurons for asynchronous state with $d_1 = 0.2$, $d_2 = 0.3$, $\omega = 0.1$ and for synchronous state with $d_1 = 0.4$, $d_2 = 0.9$, $\omega = 0.5$. As can be seen asynchronization alters the neurons waveforms from their behaviors in the absence of coupling. As Fig. 1 shows, an uncoupled neuron at the defined parameters, has fold-homoclinic (FHC) bursting behavior. FHC type bursting happens when the resting state disappears via a saddle-node bifurcation and the spiking limit cycle disappears via saddle homoclinic orbit bifurcation [14]. When we couple two neurons, in the case of synchronization, they have FHC bursting synchronization, as can be seen in the second row of Fig. 4. Whereas when they are asynchronous, their behavior is changed to the fold-Hopf (FH) bursting type, as can be seen in the first row of Fig. 4. FH type bursting occurs when the resting state disappears via saddle-node bifurcation and the limit cycle attractor shrinks to a point via supercritical Andronov–Hopf bifurcation [14].

Next we aimed to quantify synchronization global stability. Theoretical and experimental studies have proven that the neurons have coexistence of different neuronal activity regimes such as silence, tonic spiking and bursting which have significant role in dynamical memory and information processing [41]. This feature mainly depends on the initial conditions and can affect the observed synchronization pattern. So for investigating the global stability of obtained synchronous states, here we use basin stability method [11]. To compute basin stability [11], the system of coupled neurons is simulated for a large number of different random initial conditions (M). If the number of the initial conditions that lead to synchronous state, is M_s, then basin stability is calculated as M_s/M. Thus basin stability is the probability of arriving to synchronous states. If all chosen initial conditions arrive to synchronous state, basin stability will be equal to 1 and synchronization is globally stable and if basin stability is equal to zero, the synchronous state is unstable. Fig. 5 shows basin stability of the system for three different d_1 values with respect to d_1 and ω. When $d_2 = 0.2$, if d_1 increases from a threshold, the system becomes globally synchronous for high values of ω as is seen in Fig. 5(a). When d_2 is fixed at 0.5, there is a uniform basin stability for all d_1 values and synchronization is globally stable if ω increases from a threshold, as is seen in Fig. 5(b). Finally, when d_2 is raised to higher values as $d_2 = 0.8$ in Fig. 5(c), synchronization is unstable for very small d_1 values and all ω as well as $0 < d_1 < 0.4$ and ω around 0.1. Increasing d_2 decreases ω threshold at which globally stable synchronizations appear.
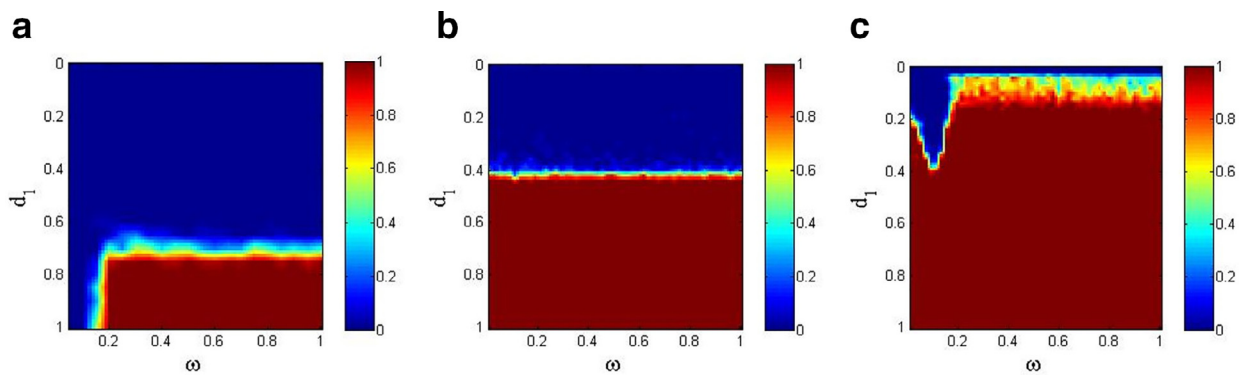
Fig. 5. Basin stability of system of Eq. (2) in ($\omega - d_1$) plane for (a) $d_2 = 0.2$, (b) $d_2 = 0.5$ and (c) $d_2 = 0.8$. The figures demonstrate that by increasing d_2 values, the system has globally stable synchronization in a wider region of ω and d_1. The color bar encodes the value of the basin stability measure.

4. Conclusion

Time-varying networks which have been studied only recently are closer to the reality specially in biology. The biological network topologies can evolve with agent dynamics as time passes. In neuronal system, synapses have the property of activity dependent changes in synaptic strength known as plasticity. Studying synchronizability and synchronization patterns in neuronal networks have significant role in neural functions and are interesting topics in neuroscience. Thus in this paper we investigated synchronization in a system of two switching coupled neurons. A modified Hindmarsh–Rose which describes the impact of electric fields in neurons was used as the model of each neuron. The extracellular electric field is always present in the living nervous system and can influence on the synaptic strength of neurons connection. Therefore, we also coupled our system through the magnetic variable to consider ephaptic coupling. At first we used the system with static coupling. We computed master stability function as a function of membrane potential coupling and ephaptic coupling to find the range of coupling strength values at which the system is synchronous. It was considered that ephaptic coupling has a negligible effect on synchronization. Whereas the membrane potential coupling variations from low to high values, enhances the synchronization possibility. Then the coupling was changed in a way that switched between two values with a frequency. The averaged synchronization error was calculated for different coupling strengths and frequencies. It was obtained that if both switching coefficient values are small, the system is asynchronous for all ω values. If one of the switching coefficients increases, then the system can be synchronous for higher frequencies. Finally large values of switching coefficients make the system synchronous for all ω values. Eventually, to check the global stability of system synchronization, the basin stability method was used and demonstrated in a parameter plane.

Competing interests

We have no competing interests.

Acknowledgment

References

[1] S. Boccaletti, G. Bianconi, R. Criado, C.I. Del Genio, J. Gómez-Gardenes, M. Romance, I. Sendina-Nadal, Z. Wang, M. Zanin, The structure and dynamics of multilayer networks, Phys. Rep 544 (2014) 1–122.
[2] S. Boccaletti, V. Latora, Y. Moreno, M. Chavez, D.-U. Hwang, Complex networks: structure and dynamics, Phys. Rep. 424 (2006) 175–308.
[3] E. Estrada, The Structure of Complex Networks: Theory and Applications, Oxford University Press, 2012.
[4] M. Kivelä, A. Arenas, M. Barthelemy, J.P. Gleeson, Y. Moreno, M.A. Porter, Multilayer networks, J. Complex Netw. 2 (2014) 203–271.
[5] S. Boccaletti, J. Kurths, G. Osipov, D. Valladares, C. Zhou, The synchronization of chaotic systems, Phys. Rep. 366 (2002) 1–101.
[6] E. Estrada, L.V. Gambuzza, M. Frasca, Synchronization in networks of Rössler oscillators with long-range interactions, in: Proceedings of the IEEE International Symposium on Circuits and Systems (ISCAS), IEEE, 2018, pp. 1–4.
[7] D. Ghosh, A.R. Chowdhury, P. Saha, On the various kinds of synchronization in delayed Duffing–Van der Pol system, Commun. Nonlinear Sci. 13 (2008) 790–803.
[8] S. Krishnagopal, J. Lehnert, W. Poel, A. Zakharova, E. Schöll, Synchronization patterns: from network motifs to hierarchical networks, Phil. Trans. R. Soc. A 375 (2017) 20160216.
[9] A. Pikovsky, M. Rosenblum, J. Kurths, J. Kurths, Synchronization: A Universal Concept in Nonlinear Sciences, Cambridge University Press, 2003.
[10] J. Ma, L. Mi, P. Zhou, Y. Xu, T. Hayat, Phase synchronization between two neurons induced by coupling of electromagnetic field, Appl. Math. Comput. 307 (2017) 321–328.
[11] S. Rakshit, A. Ray, B.K. Bera, D. Ghosh, Synchronization and firing patterns of coupled Rulkov neuronal map, Nonlinear Dyn. 94 (2018) 1–21.
[12] X. Sun, M. Perc, J. Kurths, Effects of partial time delays on phase synchronization in Watts–Strogatz small-world neuronal networks, Chaos 27 (2017) 053113.

[13] Q. Wang, M. Perc, Z. Duan, G. Chen, Synchronization transitions on scale-free neuronal networks due to finite information transmission delays, Phys. Rev. E 80 (2009) 026206.
[14] X. Sun, J. Lei, M. Perc, J. Kurths, G. Chen, Burst synchronization transitions in a neuronal network of subnetworks, Chaos 21 (2011) 016110.
[15] Q.Y Wang, Q.S. Lu, G.R. Chen, Ordered bursting synchronization and complex wave propagation in a ring neuronal network, Phys. A 374 (2007) 869–878.
[16] E. Estrada, D.J. Higham, Network properties revealed through matrix functions, SIAM Rev. 52 (2010) 696–714.
[17] S.K. Bhowmick, C. Hens, D. Ghosh, S.K. Dana, Mixed synchronization in chaotic oscillators using scalar coupling, Phys. Lett. A 376 (2012) 2490–2495.
[18] J. Ma, F. Wu, C. Wang, Synchronization behaviors of coupled neurons under electromagnetic radiation, Int. J. Mod. Phys. B 31 (2017) 1650251.
[19] M. Perc, Optimal spatial synchronization on scale-free networks via noisy chemical synapses, Biophys. Chem. 141 (2009) 175–179.
[20] L. Chen, C. Qiu, H. Huang, Synchronization with on-off coupling: role of time scales in network dynamics, Phys. Rev. E 79 (2009) 045101.
[21] M. Hasler, I. Belykh, Blinking long-range connections increase the functionality of locally connected networks, IEICE Trans. Fundam. Electr. 88 (2005) 2647–2655.
[22] R. Jeter, I. Belykh, Synchronization in on-off stochastic networks: windows of opportunity, IEEE Trans. Circuits I 62 (2015) 1260–1269.
[23] M. Porfiri, Stochastic synchronization in blinking networks of chaotic maps, Phys. Rev. E 85 (2012) 056114.
[24] M. Porfiri, D.J. Stilwell, E.M. Bollt, J.D. Skufca, Random talk: random walk and synchronizability in a moving neighborhood network, Phys. D 224 (2006) 102–113.
[25] I.V. Belykh, V.N. Belykh, M. Hasler, Blinking model and synchronization in small-world networks with a time-varying coupling, Phys. D 195 (2004) 188–206.
[26] J. Zhou, Y. Zou, S. Guan, Z. Liu, S. Boccaletti, Synchronization in slowly switching networks of coupled oscillators, Sci. Rep. 6 (2016) 35979.
[27] D.J. Stilwell, E.M. Bollt, D.G. Roberson, Synchronization of time-varying networks under fast switching, SIAM J. Appl. Dyn. Syst. 5 (2006) 140.
[28] A. Buscarino, M. Frasca, M. Branciforte, L. Fortuna, J.C. Sprott, Synchronization of two Rössler systems with switching coupling, Nonlinear Dyn. 88 (2017) 673–683.
[29] S Rakshit, B.K. Bera, D. Ghosh, Synchronization in a temporal multiplex neuronal hypernetwork, Phys. Rev. E 98 (2018) 032305.
[30] D. Cumin, C. Unsworth, Generalising the Kuramoto model for the study of neuronal synchronisation in the brain, Phys. D 226 (2007) 181–196.
[31] A. Destexhe, E. Marder, Plasticity in single neuron and circuit computations, Nature 431 (2004) 789.
[32] R.-R. Ji, C.J. Woolf, Neuronal plasticity and signal transduction in nociceptive neurons: implications for the initiation and maintenance of pathological pain, Neurobiol. Dis. 8 (2001) 1–10.
[33] N.C. Spitzer, Neurotransmitter switching? No surprise, Neuron 86 (2015) 1131–1144.
[34] S. Ge, C.-h. Yang, K.-s. Hsu, G.-l. Ming, H. Song, A critical period for enhanced synaptic plasticity in newly generated neurons of the adult brain, Neuron 54 (2007) 559–566.
[35] C.A. Anastassiou, C. Koch, Ephaptic coupling to endogenous electric field activity: why bother? Curr. Opin. Neurobiol. 31 (2015) 95–103.
[36] J. Lin, J.P Keener, Modeling electrical activity of myocardial cells incorporating the effects of ephaptic coupling, Proc. Natl. Aacd. Sci. 107 (2010) 20935–20940.
[37] H. Bokil, N. Laaris, K. Blinder, M. Ennis, A. Keller, Ephaptic interactions in the mammalian olfactory system, J. Neurosci. 21 (2001) RC173.
[38] M. Lv, C. Wang, G. Ren, J. Ma, X. Song, Model of electrical activity in a neuron under magnetic flow effect, Nonlinear Dyn. 85 (2016) 1479–1490.
[39] G. Russo, M. Di Bernardo, Contraction theory and master stability function: Linking two approaches to study synchronization of complex networks, IEEE Trans. Circuits II 56 (2009) 177–181.
[40] L.M. Pecora, T.L. Carroll, Master stability functions for synchronized coupled systems, Phys. Rev. Lett. 80 (1998) 2109.
[41] T. Malashchenko, A. Shilnikov, G. Cymbalyuk, Six types of multistability in a neuronal model based on slow calcium current, PloS One 6 (2011) e21782.